Eur. Phys. J. D **6**, 501–511 (1999)

THE EUROPEAN PHYSICAL JOURNAL D

EDP Sciences

Effect of exciton dephasing in a semiconductor microcavity

E. Brambilla[1,a], F. Castelli[1], L.A. Lugiato[1], and I. Abram[2]
[1] Dipartimento di Fisica and INFM, Via Celoria 16, 20133 Milano, Italy
[2] France Telecom/CNET, Laboratoire de Bagneux, 196 Avenue Henri Ravera, 92220 Bagneux, France

Received date: 3 June 1998 / Received in final form: 19 November 1998

Abstract. We study the interaction between delocalized excitons in a semiconductor quantum well and a longitudinal mode of the radiation field in a semiconductor microcavity with Bragg mirrors. The drastic enhancement of the spontaneous emission rate, that occurs under strong coupling conditions, is found to be surprisingly robust with respect to incoherent processes leading to dephasing of the exciton mode.

PACS. 42.55.Sa Microcavity and microdisk lasers – 42.50.Md Optical transient phenomena: quantum beats, photon echo, free-induction decay, dephasings and revivals, optical nutation, and self-induced transparency

1 Introduction

We consider a planar semiconductor microcavity, delimited by Bragg mirrors, and containing a single Quantum Well (QW), parallel to the two mirrors and placed in the middle of the planar cavity. At low temperatures and in the spectral vicinity of the QW bandgap, one can describe the radiative interaction of the QW as occurring between its delocalized Wannier excitons, and the photon modes of the cavity [1]. The translational invariance, that the system displays along the plane of the cavity and the QW, introduces a selection rule whereby each Wannier exciton of a given wave vector can interact only with the cavity photon mode that has the same component of the wave vector in the plane of the cavity. The interaction between the two quasi-particles, excitons and photons, leads to the onset of two composite modes which are called upper and lower exciton-cavity polaritons. Even in the resonant case in which the exciton and the cavity mode have the same frequency, the two polariton modes have different frequencies; this frequency splitting, which is called vacuum field Rabi splitting, has been experimentally observed in semiconductors in the early nineties [2–4]. It is considered as the signature of a "strong coupling" between the individual exciton and photon modes.

If one neglects the damping (energy dissipation) processes, the picture which emerges is that of a mutual and periodic exchange of energy between the exciton mode and the cavity mode. When the cavity mode is initially empty of photons, this exchange occurs with the vacuum field Rabi frequency. Thus, in this framework, spontaneous emission becomes a reversible process, characterized by Rabi oscillations. The passage from the weak coupling to the Rabi oscillation regimes for QW excitons embedded in cavities in which the lateral leaks of the mirrors can be ignored, has been discussed by many authors [5,6,1]

When the damping processes are taken into account, and more particularly the decay of the relevant cavity mode to the propagative radiation modes of free space, the coupling between the exciton and the cavity mode offers an important possibility for engineering spontaneous emission [7]. As observed experimentally, this allows for a drastic enhancement of the spontaneous emission decay rate [8,9]. In particular, since in microcavities the cavity mode decay rate is much faster than the spontaneous emission rate of the bare excitons, the polariton decay can be much faster than the bare exciton decay. In this way, spontaneous emission can be accelerated and this can lead to the possibility of approaching thresholdless laser emission [10].

To complete the picture, one has to take into account also the relaxation processes for the exciton. In particular, in addition to its radiative coupling to the main cavity modes, the exciton can decay radiatively by coupling to the quasi-continuum of radiation modes that correspond to the lateral cavity leaks, or it can scatter to other k-states because of phonon interactions, alloy disorder or interface roughness. These scattering processes can give rise to population decay, or simply to dephasing of an initially coherent exciton. At low temperatures, interaction with acoustic phonons is the most important source of dephasing [11,12]. The excitons dynamics and interaction with the phonons reservoir has been analyzed theoretically by several authors within microscopical models which take the QW band structure and temperature effects into account [11–16]. However, the influence of exciton dephasing at a purely phenomenological level on the cavity polariton decay has not been analyzed in much detail in the literature, apart from an examination of its effects in connection

[a] e-mail: enrico.brambilla@mi.infm.it

with exciton superradiance in a microcavity [17]. Dephasing factors which we do not take into account are inhomogeneous broadening of the excitons energy levels due to QW interface roughness [18] and many-body effects [19]. This is realistic as long as we consider high-quality samples at low temperatures. Moreover we neglect all kinds of many-body interactions since we assume we are in the low-excitation linear regime.

In this paper, we take advantage of a particular feature of the physical system, namely the large lateral leaks that are displayed by the Bragg mirrors bounding the cavity, to derive a simple model for the system of interacting excitons and photons. In this model, the different wave vector states of the two bare particles that are within the acceptance angle of the two mirrors, are lumped together and each of the bare particles is modeled as a single harmonic oscillator. Within this model, we study the problem of dephasing by adding the appropriate term to a master equation which describes the two coupled and damped oscillators, the exciton and the cavity mode.

The paper is organized as follows: In Section 2 we describe our model in terms of two coupled harmonic oscillators and review its main features. In Section 3 we formulate the master equation including exciton dephasing, and discuss its effect on the vacuum field Rabi splitting. Section 4 is devoted to the derivation of the time evolution equations which govern the decay of a single polariton, starting with the master equation. The solutions of these equations are discussed numerically and analytically in Sections 5 and 6, to illustrate the influence of dephasing on the exciton decay. Finally, Section 7 summarizes the main conclusions.

2 The model

In this section we review the basic features of the modelization of the interaction between the Wannier exciton mode and a single radiation mode in the microcavity [20]; in the low-excitation regime, the system behaves like two quantum harmonic oscillators coupled by a matrix element g.

In principle, we should distinguish a large number of exciton modes, each labelled by its wave vector k, and each interacting with a single photon mode confined in the cavity and having same in-plane wave vector. Here, however, we introduce an important simplification of the model that comes from the fact that the Bragg mirrors bounding the cavity have a relatively narrow acceptance angle θ (with respect to the normal) which is of the order of 20 degrees for GaAs/AlAs mirrors. Within this angle, the reflectivity of the mirrors is large and the photon modes are confined in the cavity. Because θ is relatively small, the frequencies of the confined photon modes are within a spread of $\pm 3\%$ of a mean frequency $\omega_{\rm ph}$, and can thus be treated as a single "lumped" photon mode of frequency $\omega_{\rm ph}$. Beyond the acceptance angle, the reflectivity of the mirrors drops to very low values and the cavity is essentially open and leaks to the ouside.

Thus, the phase space of photons can be divided into two regions. The first region includes photon wave vectors within the cone of aperture θ and corresponds to the effective "lumped" mode that is confined in the cavity, while the second region, which covers 95 % of the photon phase space includes all wave vectors outside that cone, corresponding essentially to free-space propagative modes.

Similarly, the Wannier exciton phase space is divided into three regions: The first region includes all wave vectors from $k = 0$ to $k < n(\omega_{\rm ex}/c)\sin\theta$, where n is the refractive index of the semiconductor and $\omega_{\rm ex}$ the mean exciton frequency (as the exciton dispersion is weaker than the cavity-photon dispersion we may neglect it and take a single frequency for the excitons in the first region). When the exciton is in this first region, it couples to the "lumped" photon mode confined in the planar cavity, which is detuned from the exciton frequency by a quantity $2\delta = \omega_{\rm ph} - \omega_{\rm ex}$. The second region includes all exciton wave vectors between $k > n(\omega_{\rm ex}/c)\sin\theta$ and $k < n(\omega_{\rm ex}/c)$ and corresponds to angles for which the reflectivity of the Bragg mirrors drops to a low value. When the exciton is in this second region, it does not "see" the cavity, but couples directly to the free-space modes, giving rise to ordinary spontaneous emission. Finally, the third region of phase space includes all exciton wave vectors that are larger than all possible photon wave vectors $k > n(\omega_{\rm ex}/c)$. In this region, there are no propagative photon modes to which the exciton can couple so that this region in phase space corresponds to the "dark excitons", that do not couple to light. In general, when we excite excitons through the microcavity, we access only excitons in the first region where they experience a strong coupling with the cavity modes. However, after excitation, an exciton can scatter in the two other regions through inelastic collisions with phonons.

In this simple model, neglecting momentarily the radiative coupling of excitons to the free-space photons through the cavity leaks, the system Hamiltonian can be written in the form

$$H = \hbar\omega_{\rm ex} a_1^\dagger a_1 + \hbar(\omega_{\rm ex} + 2\delta) a_2^\dagger a_2 + \hbar g(a_2^\dagger a_1 + a_1^\dagger a_2)\,, \tag{1}$$

where g is the exciton-cavity coupling constant. $a_i^\dagger$ and a_i are the creation and annihilation operators of the excitons (with $i = 1$, corresponding to excitons within the radiant manifolds, that is regions 1 and 2 of the exciton phase space) and the photons (with $i = 2$, corresponding to photons that are confined in the cavity and are in the first region of the photon phase space). The creation and annihilation operators obey the usual commutation rules for bosons:

$$[a_i, a_j^\dagger] = \delta_{ij}\,, \qquad\qquad i,j = 1,2\,.$$

The validity of this simple model rests on the fact that, because of the small acceptance angle of the Bragg mirrors and the large lateral leaks, the regions of the exciton and photon phase spaces that couple strongly to each other are very small and correspond essentially to a constant

energy, so that they can be lumped as if each consisted of a single mode.

The products of the eigenstates of $a_1^\dagger a_1$ and $a_2^\dagger a_2$ are obviously not eigenstates of H, but are relevant, since they are states with a given number of excitons and photons and form a complete set in the system Hilbert space; we denote them with $|n_1, n_2\rangle$ and we shall call them bare states in order to distinguish them from the dressed states defined below.

The coupling between the exciton and the cavity modes can be best interpreted in terms of the normal modes of Hamiltonian (1), which are mixed exciton-photon states commonly called dressed states or cavity polaritons. We first introduce the dressed-states operators A_1 and A_2 defined in order to diagonalize the Hamiltonian (1) into the simpler form

$$H = \hbar\omega_- A_1^\dagger A_1 + \hbar\omega_+ A_2^\dagger A_2 \tag{2}$$

and which simultaneously satisfy the same commutation rules as a_1 and a_2:

$$[A_i, A_j^\dagger] = \delta_{ij}\,, \qquad i,j = 1,2\,.$$

It turns out that A_1 and A_2 are related to the exciton and photon number operators by the following unitary transformation:

$$\begin{aligned} A_1 &= \alpha a_1 + \beta a_2\,, \\ A_2 &= -\beta a_1 + \alpha a_2\,, \end{aligned} \tag{3}$$

where

$$\alpha = \sqrt{\frac{\Delta+\delta}{2\Delta}}\,, \qquad \beta = \sqrt{\frac{\Delta-\delta}{2\Delta}}\,.$$

$\omega_\pm$ are given by

$$\omega_\pm = \frac{\omega_{\rm ex}+\omega_{\rm ph}}{2} \pm \sqrt{g^2+\delta^2} = \omega_{\rm ex} + \delta \pm \Delta \tag{4}$$

and are called polariton frequencies;

$$2\Delta = \omega_+ - \omega_- = 2\sqrt{g^2+\delta^2}$$

is the Rabi splitting produced by the exciton-photon interaction. The dressed states are thus eigenstates of the number operators $A_1^\dagger A_1$ and $A_2^\dagger A_2$, and can be denoted as $|N_1, N_2\rangle'$. They can therefore be seen as states with N_1 polaritons in the lower energy level $\hbar\omega_-$ and N_2 polaritons in the upper energy level $\hbar\omega_+$ (in the following we will call them lower and upper polaritons). Calling the two lowest excited states $|L\rangle = |1,0\rangle'$ and $|U\rangle = |0,1\rangle'$ we have from equation (3)

$$\begin{aligned} |00\rangle' &= |00\rangle\,, \\ |L\rangle &= \alpha|1,0\rangle + \beta|0,1\rangle\,, \\ |U\rangle &= -\beta|1,0\rangle + \alpha|0,1\rangle\,. \end{aligned} \tag{5}$$

3 The master equation

In a real cavity both the exciton and the photon modes are coupled to a spectral continuum of modes which leads to dissipation. In addition, excitons are subject to incoherent processes, both elastic and inelastic, whose net effect is dephasing (*i.e.* a redistribution of the excitonic population in k-space). Taking into account these processes in the framework of the Markovian approximation, the system dynamics can be described by the following master equation for the density operator ρ:

$$\begin{aligned} \frac{{\rm d}\rho}{{\rm d}t} &= \frac{1}{i\hbar}[H,\rho] \\ &+ \kappa_{\rm ph}\left\{[a_2, \rho a_2^\dagger] + [a_2\rho, a_2^\dagger]\right\} \\ &+ \gamma_{\rm ex}\left\{[a_1, \rho a_1^\dagger] + [a_1\rho, a_1^\dagger]\right\} \\ &+ \gamma_\phi\left\{[a_1^\dagger a_1, \rho a_1^\dagger a_1] + [a_1^\dagger a_1\rho, a_1^\dagger a_1]\right\}. \end{aligned} \tag{6}$$

The first term describes, of course, the free evolution of the strongly coupled system in the absence of any relaxation processes.

The second term, which is proportional to $\kappa_{\rm ph}$, describes the photon losses through the cavity mirrors, $\kappa_{\rm ph}$ being the cavity damping constant for the electric field amplitude.

The third term describes the overall exciton decay, $\gamma_{\rm ex}$ being the decay rate for the exciton amplitude. It must be understood as the inverse of the exciton decay time $2T_1$, well known in the literature, and takes into account different contributions. One is the radiative recombination in off-axial directions, that is spontaneous emission through the lateral leaks of the Bragg mirrors, corresponding to the radiative coupling of excitons to the second region of the photon phase space. The other contribution is inelastic scattering to the dark states of phase space (the region of phase space that corresponds to wave vectors that are much longer than the photon wave vector, as discussed in Section 2). A review of the different processes that photoexcited excitons undergo in quantum wells has been given by Andreani [21] and by Citrin [22]. In general, for $T > 10$ K exciton thermalisation and scattering to dark states are faster than the intrinsic radiative decay rate which means that, at these temperatures, $\gamma_{\rm ex}$ is dominated essentially by the scattering rate to the dark states. We note that because strong coupling occurs in a very small region of phase space, the rest of phase space conserves essentially the same structure and the same interactions as for free excitons, and for this reason $\gamma_{\rm ex}$ can be taken to be the total free-exciton decay rate to a good approximation.

The last term takes account of the phase destroying processes due to scattering involving excitons, but not already included in $\gamma_{\rm ex}$ [23]; the dephasing coefficient γ_ϕ corresponds to the inverse of the pure dephasing time T_2^*. It must be noticed that the quantities measured in experiments are usually the exciton decay time T_1, and the total

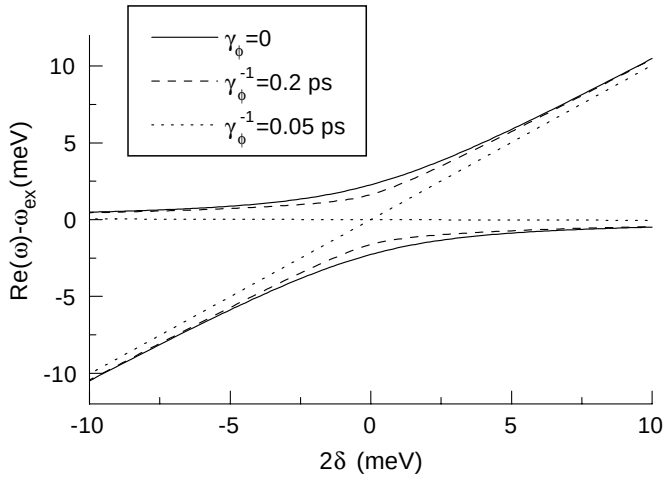

Fig. 1. $\mathrm{Re}(\overline{\omega}_{\pm}) - \omega_{\mathrm{ex}}$ plotted as functions of the detuning parameter 2δ. The full lines correspond to the conservative system with $\gamma_{\mathrm{ex}} = \kappa_{\mathrm{ph}} = \gamma_{\phi} = 0$ and $2g = 4.5$meV. The dashed lines are plotted for increasing values of the dephasing rate, with $\tau_{\mathrm{ex}} = 12$ ps and $\tau_{\mathrm{ph}} = 2$ ps.

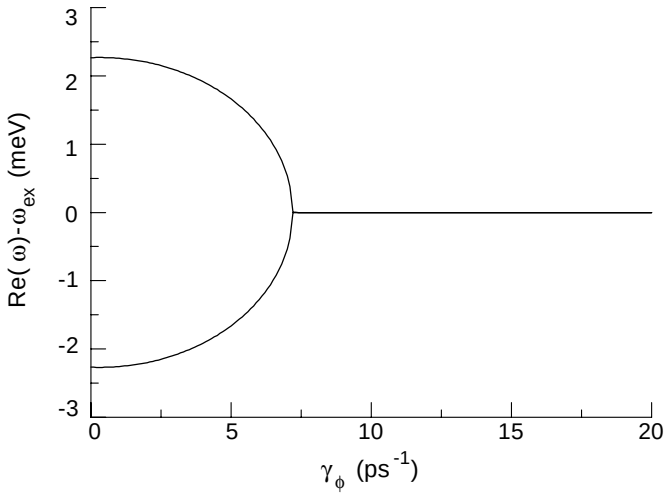

Fig. 2. $\mathrm{Re}(\overline{\omega}_{\pm}) - \omega_{\mathrm{ex}}$ plotted as functions of γ_{ϕ} in the resonant case for $\tau_{\mathrm{ex}} = 12$ ps, $\tau_{\mathrm{ph}} = 2$ ps and $2g = 4.5$ meV. They vanish for $\gamma_{\phi} > 2g - \gamma_{\mathrm{ex}} + \kappa_{\mathrm{ph}} \simeq 7$ ps^{-1}.

dephasing time $1/T_2 = 1/(2T_1) + 1/T_2^*$; however, in our analysis we will consider T_1 and T_2^*, rather than T_1 and T_2, as independent parameters.

For excitons, the physical processes that lead to dephasing are essentially the same as those that produce scattering to dark states: phonon interactions, alloy disorder, impurity and defect scattering, well-width fluctuations, interface roughness, etc. The distinction between dephasing and population decay for our exciton system is simply a matter of extent: in dephasing processes the exciton stays within the radiant region of phase space and is always coupled to the electromagnetic field either in terms of strong coupling to the confined cavity modes or in terms of dissipative coupling to the external photon continuum through the lateral leaks of the Bragg mirrors. In this way, the expectation value of the exciton number operator $a_1^{\dagger}a_1$ remains unchanged. If excitons are scattered to the dark states, they no longer belong to the population that can interact with the electromagnetic field and, in doing the bookkeeping, these processes contribute to the decay of the diagonal elements of the density matrix and are included in γ_{ex}.

Alternatively, the physical meaning of the two terms of equation (6) that refer to the "excitonic" harmonic oscillator, becomes more transparent with the help of the following consideration. If we consider formally only the excitonic part, then the master equation reduces to

$$\frac{\mathrm{d}\rho_{\mathrm{ex}}}{\mathrm{d}t} = \gamma_{\mathrm{ex}} \left\{ [a_1, \rho a_1^{\dagger}] + [a_1 \rho, a_1^{\dagger}] \right\} + \gamma_{\phi} \left\{ [a_1^{\dagger}a_1, \rho a_1^{\dagger}a_1] + [a_1^{\dagger}a_1 \rho, a_1^{\dagger}a_1] \right\}, \quad (7)$$

where ρ_{ex} is the density matrix for the excitonic part only. If now we introduce the P-function [24] such that

$$\rho_{\mathrm{ex}}(t) = \int \mathrm{d}^2\alpha P(\alpha, \alpha^*, t) |\alpha\rangle\langle\alpha|, \quad (8)$$

where $|\alpha\rangle$ is the generic coherent state of the harmonic oscillator, and express the c-number α as $\alpha = r\exp(i\phi)$, equation (7) leads to the following Fokker-Planck equation for $P(r, \phi, t)$ [23]:

$$\frac{\partial P(r,\phi,t)}{\partial t} = \gamma_{\mathrm{ex}} \frac{1}{r} \frac{\partial}{\partial r} r^2 P + \gamma_{\phi} \frac{\partial^2 P}{\partial \phi^2}. \quad (9)$$

Clearly, the part of the master equation proportional to γ_{ex} leads to a pure drift term which contributes to both diagonal and non-diagonal terms of the density matrix, whereas the part proportional to γ_{ϕ} leads to a pure diffusive term (dephasing) that, in particular, contributes to the decay of the off-diagonal term elements only.

From equation (6) we can derive the equations for the mean values of the mode amplitudes $\langle a_1 \rangle = \mathrm{Tr}(a_1\rho)$ and $\langle a_2 \rangle = \mathrm{Tr}(a_2\rho)$:

$$\frac{\mathrm{d}}{\mathrm{d}t}\langle a_1 \rangle = -i\omega_{\mathrm{ex}}\langle a_1 \rangle - ig\langle a_2 \rangle - (\gamma_{\mathrm{ex}} + \gamma_{\phi})\langle a_1 \rangle,$$

$$\frac{\mathrm{d}}{\mathrm{d}t}\langle a_2 \rangle = -i(\omega_{\mathrm{ex}} + 2\delta)\langle a_2 \rangle - ig\langle a_1 \rangle - \kappa_{\mathrm{ph}}\langle a_2 \rangle. \quad (10)$$

Searching for a solution of the form $\langle a_i \rangle \propto e^{-i\omega t}$, we find the two complex frequencies

$$\overline{\omega}_{\pm} = \frac{\omega_{\mathrm{ex}} + \omega_{\mathrm{ph}}}{2} + \delta - \frac{i}{2}(\gamma_{\mathrm{ex}} + \kappa_{\mathrm{ph}} + \gamma_{\phi}) \pm \frac{1}{2}\sqrt{[2\delta + i(\gamma_{\mathrm{ex}} + \gamma_{\phi} - \kappa_{\mathrm{ph}})]^2 + 4g^2}. \quad (11)$$

For $\gamma_{\phi} = 0$ this coincides with the result found by Yamamoto *et al.* [25]. Setting $\gamma_{\mathrm{ex}} = \kappa_{\mathrm{ph}} = \gamma_{\phi} = 0$ in equation (11), that is by considering the ideal undamped system, we find the energy eigenvalues $E^{\pm} = \hbar\omega_{\pm}$ of the

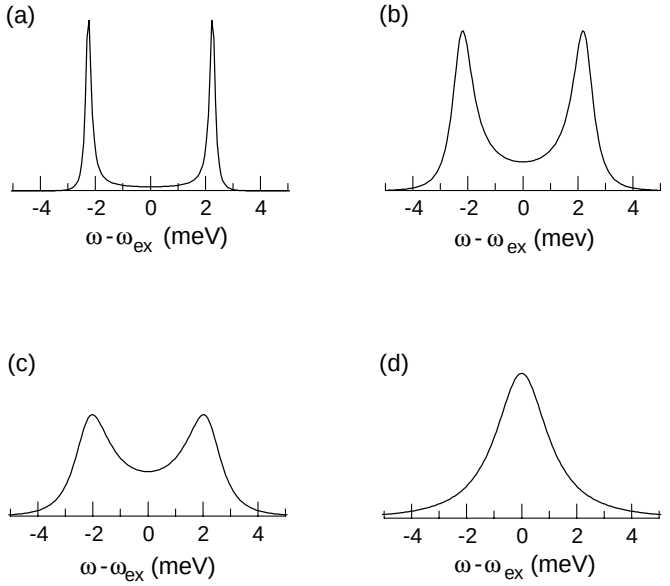

Fig. 3. The spectrum in the resonant case for $\gamma_\phi = 0$ (a), $\gamma_\phi^{-1} = 1$ (b), $\gamma_\phi^{-1} = 0.5$ ps (c), $\gamma_\phi^{-1} = 0.1$ ps (d). The other parameters are the same as in the previous figures: $\tau_{\rm ex} = 12$ ps, $\tau_{\rm ph} = 2$ ps and $2g = 4.5$ meV.

conservative system (1), $\omega_\pm$ being the upper and lower polariton frequencies given by equation (4).

In Figure 1 $\mathrm{Re}(\overline{\omega}_\pm - \omega_{\rm ex})$ are plotted as a function of the detuning δ for the set of parameters corresponding to the experiment of Abram *et al.* [8,9], but for different values of γ_ϕ: we set $\tau_{\rm ex} = (2\gamma_{\rm ex})^{-1} = 12$ ps, $\tau_{\rm ph} = (2\kappa_{\rm ph})^{-1} = 2$ ps for the free exciton and the photon decay rates, and $2g = 4.5$ meV for the coupling constant. The full line corresponds to the case of pure polariton states (*i.e.* with $\gamma_{\rm ex} = \kappa_{\rm ph} = \gamma_\phi = 0$); the dashed lines correspond to real cases with nonzero dissipation constants, and show the progressive deterioration of the polariton states due to the increasing of dephasing.

The quantities $\mathrm{Re}(\overline{\omega}_\pm - \omega_{\rm ex})$ are also plotted as a function of γ_ϕ in the resonant case (*i.e.* for $\delta = 0$, $\omega_{\rm ex} = \omega_{\rm ph}$) in Figure 2; we see from equation (11) that they vanish for $\gamma_{\rm ex} + \gamma_\phi - \kappa_{\rm ph} > 2g$.

In general, the description of the system in terms of the dressed states defined by equation (5) is best suited when the dissipation constants are small with respect to the Rabi constant g. In such a case the existence of the cavity polariton modes manifests itself in the frequencies domain in the form of a doublet separated by the Rabi splitting 2Δ [2], and has also been observed experimentally in the time domain in the form of damped Rabi oscillations of the emitted field [25,26]. The spectral distribution of the emitted radiation is defined as the Fourier transform of the two-time correlation function of the field. For the case of ergodic and stationary processes this function is simply proportional to $\langle a_2^\dagger(t) a_2(0)\rangle$ and, by making use of the quantum regression theorem [27], one finds (see Eq. (15) of ref. [25]):

$$\begin{aligned} S(\omega) &= \int_0^\infty \langle a_2^\dagger(t) a_2(0)\rangle e^{-i\omega t} \mathrm{d}t + \mathrm{c.c.} \\ &= \frac{A^\dagger}{(\omega - \mathrm{Re}(\overline{\omega}_+))^2 + \mathrm{Im}(\overline{\omega}_+)^2} + \\ &\quad + \frac{A^-}{(\omega - \mathrm{Re}(\overline{\omega}_-)^2 + \mathrm{Im}(\overline{\omega}_-)^2}\,, \end{aligned} \tag{12}$$

where $\overline{\omega}_\pm$ are given by equation (11). $A^\pm$ are only slowly varying function of ω near the denominator minimum and can thus be considered as constants. We have therefore two Lorentzian shaped peaks of width $\mathrm{Im}(\overline{\omega}_-)$ and $\mathrm{Im}(\overline{\omega}_+)$, approximately centered on $\mathrm{Re}(\overline{\omega}_-)$ and $\mathrm{Re}(\overline{\omega}_+)$.

Figure 3 plots $S(\omega)$ in the resonant case for increasing values of the dephasing coefficient γ_ϕ (the peaks are symmetric with respect to $\omega_{\rm ex} + \omega_{\rm ph}/2$ only when $\delta = 0$). The spectral doublet is clearly distinguishable (Fig. 3a, b) as long as γ_ϕ remains small with respect to the Rabi coupling constant g and its experimental observation gives evidence of the Rabi oscillations of the emitted fields. When γ_ϕ (or, alternatively, $\gamma_{\rm ex}$ or $\kappa_{\rm ph}$) becomes of the same order of magnitude as g or greater, the doublet disappears (Fig. 3c, d).

4 The population equations

Using the master equation (6) we can obtain an equivalent set of infinite coupled linear equations for the density matrix elements, both in the bare-states and in the dressed-states picture. Setting $\rho_{n_1' n_2' n_1 n_2} \equiv \langle n_1' n_2' | \rho | n_1 n_2 \rangle$ for the bare states and assuming that initially there is only one exciton, we will only consider the ground state $|00\rangle$ and the first two excited states $|10\rangle$ and $|01\rangle$, thus obtaining the following rate equations:

$$\begin{aligned} \frac{\mathrm{d}\rho_{00}}{\mathrm{d}t} &= 2\gamma_{\rm ex}\rho_{10} + 2\kappa_{\rm ph}\rho_{01}\,, \\ \frac{\mathrm{d}\rho_{10}}{\mathrm{d}t} &= -2\gamma_{\rm ex}\rho_{10} + ig(\rho_{1001} - \rho_{0110})\,, \\ \frac{\mathrm{d}\rho_{01}}{\mathrm{d}t} &= -2\kappa_{\rm ph}\rho_{01} - ig(\rho_{1001} - \rho_{0110})\,, \\ \frac{\mathrm{d}\rho_{1001}}{\mathrm{d}t} &= -(\gamma_{\rm ex} + \kappa_{\rm ph} + \gamma_\phi - 2i\delta)\rho_{1001} + ig(\rho_{10} - \rho_{01})\,, \\ \frac{\mathrm{d}\rho_{0110}}{\mathrm{d}t} &= -(\gamma_{\rm ex} + \kappa_{\rm ph} + \gamma_\phi + 2i\delta)\rho_{0110} - ig(\rho_{10} - \rho_{01})\,, \end{aligned} \tag{13}$$

where the diagonal matrix elements $\rho_{n_1 n_2} \equiv \rho_{n_1 n_2 n_1 n_2}$ are the bare-states occupation probabilities. In the low-excitation regime ρ_{00}, ρ_{10} and ρ_{01} are proportional to the populations of the ground state, the one-exciton state and the one-photon state, respectively. On the other hand, we define the density matrix in the dressed-state picture $p_{N_1' N_2' N_1 N_2} = \langle N_1' N_2' | \rho | N_1 N_2 \rangle'$ and we get the following

rate equations:

$$\begin{aligned}
\frac{\mathrm{d}p_{00}}{\mathrm{d}t} &= 2\gamma_1 p_{10} + 2\gamma_2 p_{01} - 2\tilde{\gamma}(p_{1001} + p_{0110})\,,\\
\frac{\mathrm{d}p_{10}}{\mathrm{d}t} &= -\left(2\gamma_1 + \gamma_\phi \frac{g^2}{2\Delta^2}\right) p_{10} + \gamma_\phi \frac{g^2}{2\Delta^2} p_{01}\,,\\
&\quad + \left(\tilde{\gamma} - \gamma_\phi \frac{g\delta}{2\Delta^2}\right)(p_{1001} + p_{0110})\,,\\
\frac{\mathrm{d}p_{01}}{\mathrm{d}t} &= -\left(2\gamma_2 + \gamma_\phi \frac{g^2}{2\Delta^2}\right) p_{01} + \gamma_\phi \frac{g^2}{2\Delta^2} p_{10}\,,\\
&\quad + \left(\tilde{\gamma} + \gamma_\phi \frac{g\delta}{2\Delta^2}\right)(p_{1001} + p_{0110})\,,\\
\frac{\mathrm{d}p_{1001}}{\mathrm{d}t} &= -\left(\gamma_{\mathrm{ex}} + \kappa_{\mathrm{ph}} + \gamma_\phi\left(1 - \frac{g^2}{2\Delta^2}\right) - 2i\Delta\right) p_{1001}\,,\\
&\quad + \gamma_\phi \frac{g^2}{2\Delta^2} p_{0110} + \left(\tilde{\gamma} - \gamma_\phi \frac{g\delta}{2\Delta^2}\right) p_{10}\,,\\
&\quad + \left(\tilde{\gamma} + \gamma_\phi \frac{g\delta}{2\Delta^2}\right) p_{01}\,,\\
\frac{\mathrm{d}p_{0110}}{\mathrm{d}t} &= -\left(\gamma_{\mathrm{ex}} + \kappa_{\mathrm{ph}} + \gamma_\phi\left(1 - \frac{g^2}{2\Delta^2}\right) + 2i\Delta\right) p_{0110}\,,\\
&\quad + \gamma_\phi \frac{g^2}{2\Delta^2} p_{1001} + \left(\tilde{\gamma} - \gamma_\phi \frac{g\delta}{2\Delta^2}\right) p_{10}\,,\\
&\quad + \left(\tilde{\gamma} + \gamma_\phi \frac{g\delta}{2\Delta^2}\right) p_{01}\,, \qquad (14)
\end{aligned}$$

where

$$\begin{aligned}
\gamma_1 &= \alpha^2\gamma_{\mathrm{ex}} + \beta^2\kappa_{\mathrm{ph}}\,,\\
\gamma_2 &= \alpha^2\kappa_{\mathrm{ph}} + \beta^2\gamma_{\mathrm{ex}}\,,\\
\tilde{\gamma} &= \alpha\beta(\gamma_{\mathrm{ex}} - \kappa_{\mathrm{ph}})\,. \qquad (15)
\end{aligned}$$

We assume that the initial state is a one-polariton state, or a linear combination of the two one-polariton states, so that all the other matrix elements can be neglected. The unitary transformation relating the density matrix elements in the two pictures can then be calculated from equations (3) and (5):

$$\begin{pmatrix} p_{00}\\ p_{10}\\ p_{01}\\ p_{1001}\\ p_{0110}\end{pmatrix} = \begin{pmatrix} 1 & 0 & 0 & 0 & 0\\ 0 & \alpha^2 & \beta^2 & \alpha\beta & \alpha\beta\\ 0 & \beta^2 & \alpha^2 & -\alpha\beta & -\alpha\beta\\ 0 & -\alpha\beta & \alpha\beta & \alpha^2 & -\beta^2\\ 0 & -\alpha\beta & \alpha\beta & -\beta^2 & \alpha^2\end{pmatrix} \begin{pmatrix} \rho_{00}\\ \rho_{10}\\ \rho_{01}\\ \rho_{1001}\\ \rho_{0110}\end{pmatrix}. \qquad (16)$$

5 Influence of dephasing on the exciton decay

The presence of dephasing shortens the polariton lifetime, in general. A more detailed study of the influence of dephasing on the radiative decay rate has been done both numerically, by direct integration of the population equations (14), and analytically, by solving the associated characteristic equation for the eigenvalues in some particular cases.

In this view we briefly recall the results obtained in the absence of dephasing. Let us consider first the resonant case. For $\gamma_\phi = 0$, $\delta = 0$, equations (14) (or, equivalently, Eq. (13)) have the five eigenvalues

$$\begin{aligned}
&\lambda = 0, \qquad \lambda = \gamma_{\mathrm{ex}} + \kappa_{\mathrm{ph}} \ \text{(double)}\,,\\
&\lambda_{1,2} = \gamma_{\mathrm{ex}} + \kappa_{\mathrm{ph}} \pm \sqrt{(\gamma_{\mathrm{ex}} - \kappa_{\mathrm{ph}})^2 - 4g^2}\,. \qquad (17)
\end{aligned}$$

The eigenvalue $\lambda = 0$ concerns only the population of the ground state and does not affect the decay. The last couple of eigenvalues, in which 1 (2) corresponds to + (−), respectively, makes the difference between the strong-coupling and the weak-coupling case. In the weak-coupling case $g \ll \gamma_{\mathrm{ex}}, \kappa_{\mathrm{ph}}$ one has

$$\lambda_1 \simeq 2\gamma_{\mathrm{ex}}\,, \qquad \lambda_2 \simeq 2\kappa_{\mathrm{ph}}\,. \qquad (18)$$

Hence if $\gamma_{\mathrm{ex}} \ll \kappa_{\mathrm{ph}}$, as is usual, the decay is governed by the rate $2\gamma_{\mathrm{ex}}$, which is the slowest decay rate in play. On the other hand, in the strong-coupling case $g \gg \gamma_{\mathrm{ex}}, \kappa_{\mathrm{ph}}$ one has $\lambda_{1,2} \simeq \gamma_{\mathrm{ex}} + \kappa_{\mathrm{ph}} \pm 2ig$. The decay rate is thus

$$\gamma_{\mathrm{ex}} + \kappa_{\mathrm{ph}}\,, \qquad (19)$$

so that if $\kappa_{\mathrm{ph}} \gg \gamma_{\mathrm{ex}}$, the emission rate of the dressed exciton is much larger than the free-exciton decay rate $2\gamma_{\mathrm{ex}}$ as is well known.

Out of resonance, when the detuning becomes large with respect to g, the photon-exciton coupling becomes less effective, and one expects that the exciton and the photon modes decay independently with their respective decay rates $2\gamma_{\mathrm{ex}}$ and $2\kappa_{\mathrm{ph}}$. This is explained by the following reasosning. Let us assume that the system is initially in one of the dressed state $|L\rangle$ or $|U\rangle$; for short times, the decay is given by the coefficient of p_{10} and p_{01}, respectively, in the second and the third of equations (14). For $\gamma_\phi = 0$ they are

$$\begin{aligned}
2\gamma_1 &= 2\left\{\frac{\Delta + \delta}{2\Delta}\gamma_{\mathrm{ex}} + \frac{\Delta - \delta}{2\Delta}\kappa_{\mathrm{ph}}\right\},\\
2\gamma_2 &= 2\left\{\frac{\Delta - \delta}{2\Delta}\gamma_{\mathrm{ex}} + \frac{\Delta + \delta}{2\Delta}\kappa_{\mathrm{ph}}\right\}; \qquad (20)
\end{aligned}$$

these expressions have been used in [8,9] to fit the experimental data. One can control spontaneous emission by varying the cavity decay rate κ_{ph}, or the detuning δ. In the limit of large positive δ (so that $\Delta \simeq \delta$) one has $\gamma_1 \simeq \gamma_{\mathrm{ex}}$, $\gamma_2 \simeq \kappa_{\mathrm{ph}}$ and one recovers the bare-exciton decay rate for the lower polariton (γ_1). For large negative δ (so that $\Delta \simeq -\delta$) one has, conversely, $\gamma_1 \simeq \kappa_{\mathrm{ph}}$, $\gamma_2 \simeq \gamma_{\mathrm{ex}}$.

We now consider the general case with nonzero values of γ_ϕ. For the sake of clarity we suppose that the system is initially excited into the lower polariton state $|L\rangle$ and we solve numerically equations (14) with a fourth-order Runge-Kutta routine. Figures 4 a,b,c show the population dynamics for increasing values of the dephasing coefficient γ_ϕ, as calculated under strong coupling conditions (with $2g = 4.5$ meV).

When γ_ϕ is negligible or zero and the strong coupling condition holds, we see that the excited polariton state

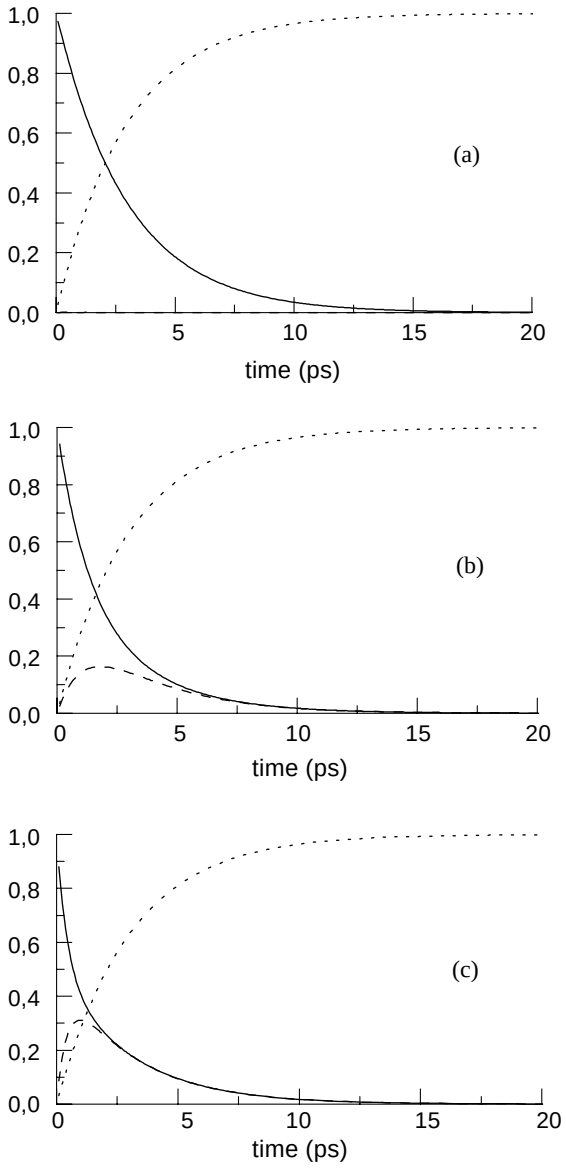

Fig. 4. The populations of the two polariton states $|L\rangle$ (solid line, p_{10}) and $|U\rangle$ (broken line, p_{01}) and that of the ground state (dotted line, p_{00}) plotted as functions of time in the resonant case for $\gamma_\phi = 0$ (a), $\gamma_\phi^{-1} = 2$ ps (b) and $\gamma_\phi^{-1} = 0.5$ ps (c). The other parameters are the same as in the previous figures.

decays directly on the ground state while the level $|U\rangle$ remains practically unoccupied during the entire system dynamics (Fig. 4a). In this situation the polariton states remain indeed well defined and, in the resonant case, the spontaneous emission characteristic time is of the order $(\gamma_{\rm ex} + \kappa_{\rm ph})^{-1} \simeq \kappa_{\rm ph}^{-1} \simeq 3$ ps, in agreement with equation (19). For larger values of γ_ϕ (Figs. 4b, c), in times of the order of γ_ϕ^{-1}, there is a buildup of probability of finding one upper polariton when initially there is only one lower polariton, without a change of the total energy of the system. Hence there is admixture of the two polaritons and this is the main effect of dephasing for the dynamics of the probabilities.

One can clearly distinguish two stages in the time evolution. In the first stage the dephasing gives rise to a redistribution of the populations of the two polariton states, in the second stage the polaritons simultaneously decay to the ground state. The separation between the two stages becomes clearest when γ_ϕ is larger than g, $\kappa_{\rm ph}$ and $\gamma_{\rm ex}$. However, it is appropriate to analyze the two stages separately in any case.

5.1 Initial polariton decay rate

For short times the decay rate is given, again, by the coefficient of p_{10} and p_{01} in the second and third of equations (14), depending on which state, $|L\rangle$ or $|U\rangle$, we start from. The corresponding characteristic times τ_L and τ_U are thus given by

$$\tau_L^{-1} = 2\gamma_1 + \gamma_\phi \frac{g^2}{2\Delta^2} \tag{21}$$

and

$$\tau_U^{-1} = 2\gamma_2 + \gamma_\phi \frac{g^2}{2\Delta^2}\,. \tag{22}$$

For $\delta = 0$ the two coincide whereas for $\delta \neq 0$ they become strongly different. Figure 5 shows τ_L and τ_U as a function of δ for $\gamma_\phi = 0$ and $\gamma_\phi^{-1} = 0.1$ ps, under strong-coupling conditions. When γ_ϕ^{-1} becomes shorter than 1 ps, the two curves exhibit a minimum for $\delta = 0$.

5.2 Decay to the ground state

Insight on the population dynamics in this stage can be gained by direct evaluation of the smallest eigenvalues of equations (13) (or Eqs. (14)). In general, the characteristic equation is a fourth-order equation which must be solved numerically (we neglect the trivial eigenvalue $\lambda = 0$ which is always present). However, in the case of large dephasing, *i.e.* when

$$\gamma_\phi \gg g, \gamma_{\rm ex}, \kappa_{\rm ph}\,, \tag{23}$$

equations (14) have a pair of complex conjugate eigenvalues whose real part is of the same order as γ_ϕ, which determine the short time scale dynamics due to dephasing, and two real eigenvalues of the same order as $\gamma_{\rm ex}$ and $\kappa_{\rm ph}$, which determine the decay rate of the populations to the ground state. In this situation approximate expressions for the two smallest eigenvalues λ_- and λ_+ can be found in a straightforward way by adiabatic elimination of the nondiagonal matrix elements ρ_{1001} and ρ_{0110} in equations (13); we obtain

$$\lambda_\pm^{\rm ap}(\delta) = \gamma_{\rm ex} + \kappa_{\rm ph} + R(\delta) \pm \sqrt{(\gamma_{\rm ex} - \kappa_{\rm ph})^2 + R(\delta)^2} \tag{24}$$

with

$$R(\delta) = \frac{2g^2\gamma_\phi}{\gamma_\phi^2 + 4\delta^2}\,.$$

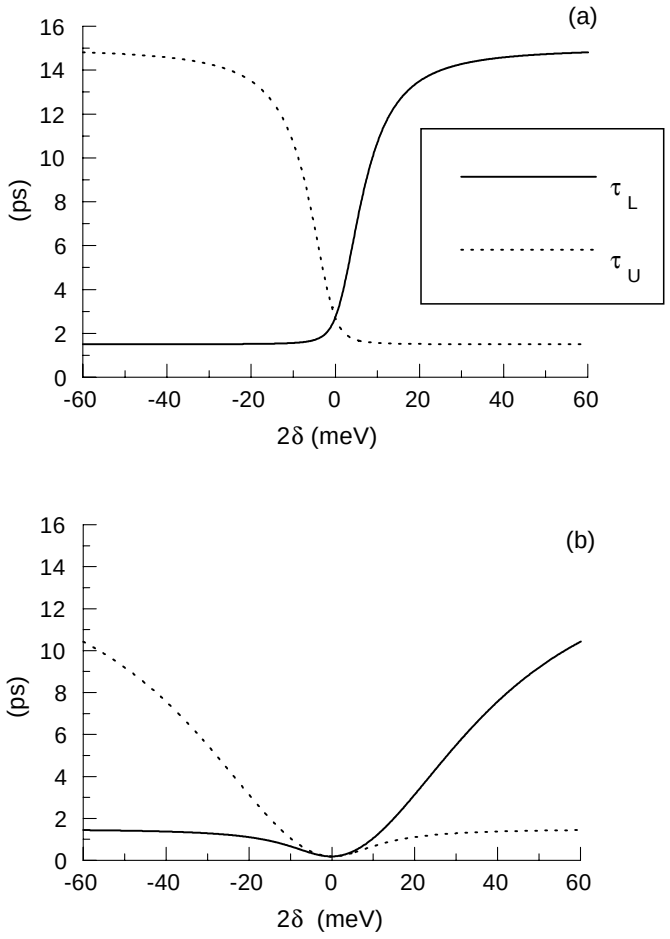

Fig. 5. The two initial decay times τ_L (solid line) and τ_U (broken line) are plotted as a function of the detuning 2δ for $\gamma_\phi = 0$ (a) and $\gamma_\phi^{-1} = 0.1$ ps (b). The other parameters are the same as in the previous figures

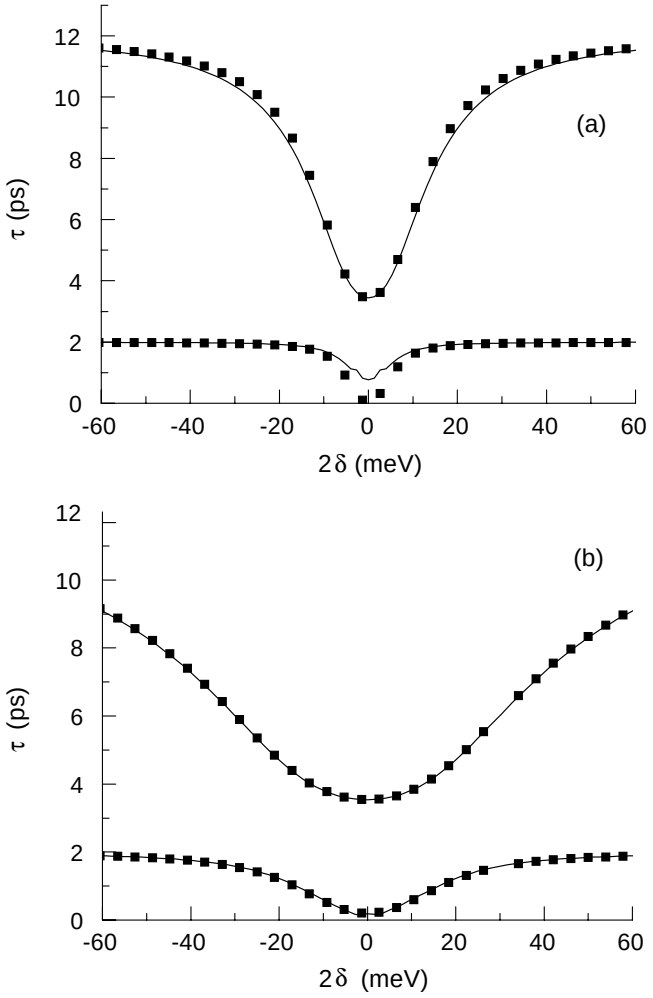

Fig. 6. $(\mathrm{Re}(\lambda_\pm))^{-1}$ as a function of the detuning parameter 2δ, for $\gamma_\phi^{-1} = 1$ ps (a) and $\gamma_\phi^{-1} = 0.1$ ps (b). The solid line corresponds to the approximated expression given by equation (21) while the points are calculated by solving numerically the eigenvalue equation. The other parameters are the same as in Figure 3.

Figure 6 shows the plot of the numerical and the approximate analytical values (24) of $\lambda_\pm^{-1}$ as functions of δ under strong-coupling conditions, for $\gamma_\phi^{-1} = 1$ ps (a) and $\gamma_\phi^{-1} = 0.1$ ps (b). Of course, equation (24) is a good approximation also under weak-coupling conditions, *i.e.* when g is comparable with γ_{ex} and κ_{ph}, the essential condition for its validity being a large value of the dephasing coefficient γ_ϕ. Note that $\lambda_\pm^{-1}$ given by equation (24) are even functions of δ, contrary to the curves of τ_L and τ_U (see Eqs. (21), (22)) which are symmetrical with respect to each other (Fig. 5).

Let us now consider in more detail the resonant case $\delta = 0$. Of the five eigenvalues of equations (13) (or Eqs. (14)) one is $\lambda = 0$, another is $\lambda = \gamma_{\mathrm{ex}} + \kappa_{\mathrm{ph}} + \gamma_\phi$, and the remaining three obey a cubic equation. For large γ_ϕ the decay to the ground state is determined by the roots of the cubic equation, or more precisely, by the two solutions which are approximated by λ_+^{ap} and λ_-^{ap}. Figure 7 shows the inverse of the real parts of the three roots of the cubic equation labeled as 1, 2, 3 for a wide range of γ_ϕ under strong-coupling conditions, and compares them with $(\lambda_\pm^{\mathrm{ap}})^{-1}$, which are indicated as squares. It can be seen that λ_-^{ap} fits very well the found numerical value even when γ_ϕ becomes negligible. This can be understood by noting that

$$\lambda_-^{\mathrm{ap}}(\delta = 0) \overset{\gamma_\phi \to 0}{\longrightarrow} \gamma_{\mathrm{ex}} + \kappa_{\mathrm{ph}}$$

in agreement with equation (19). Actually, it turns out that under strong-coupling conditions the analytical approximation $\lambda_-^{\mathrm{ap}}(\delta)$ is usually a good approximation to the exact numerical result; this is important because the decay to the ground state is really governed by the rate λ_-^{-1}, since λ_- is the eigenvalue with the smallest real part. In the weak-coupling case the analytical expressions (24) hold only when γ_ϕ is large enough and the corresponding exact eigenvalues are practically constant and equal to the bare decay rates $2\gamma_{\mathrm{ex}}$ and $2\kappa_{\mathrm{ph}}$.

Also in the strong-coupling case, but under condition of large detuning, the decay rates are $2\gamma_{\mathrm{ex}}$ and $2\kappa_{\mathrm{ph}}$, as one sees from equations (24).

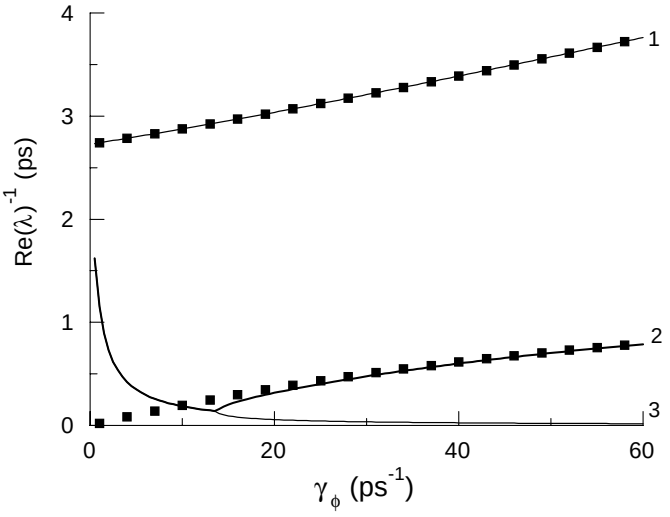

Fig. 7. Resonant case. The inverse of the real part of the three solutions of the cubic eigenvalue equation of the resonant case are plotted as a function of γ_ϕ under strong-coupling conditions ($2g = 4.5$ meV). The squares correspond to the approximate expression given by equation (24) while the full lines are calculated numerically. The other parameters are the same as in Figure 3.

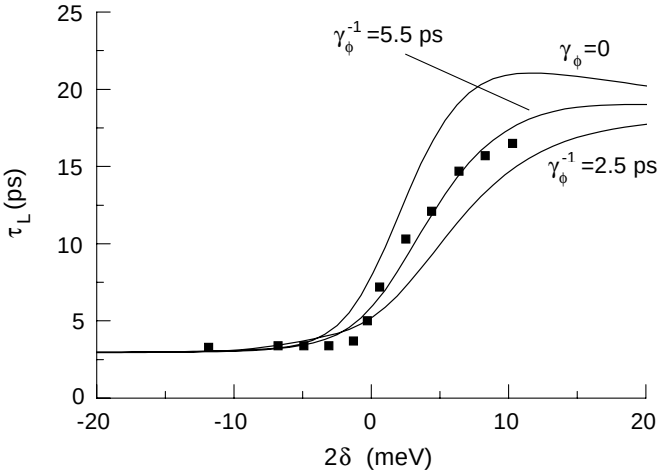

Fig. 8. Calculated decay time of the lower polariton for different values of the dephasing time (solid lines). The calculated curve is convoluted with the experimental response function, corresponding to a resolution of 3 ps. The best fit to the experimental values (squares) is obtained for $\gamma_\phi^{-1} = 5.5$ ps. The other parameters are $\tau_{\rm ex} = 12$ ps, $\tau_{\rm ph} = 2$ ps and $2g = 4.5$ meV.

The most interesting result arises in the resonant case under strong-coupling conditions. If we look at Figure 7, we see that the decay time λ_-^{-1}, which governs the decay to the ground state, remains practically equal to $(\gamma_{\rm ex} + \kappa_{\rm ph})^{-1}$ for moderate dephasing (*i.e.* $\gamma_\phi < g$), and even for very strong dephasing ($\gamma_\phi^{-1} = 0.1$ ps) it remains of the same order as $(\gamma_{\rm ex} + \kappa_{\rm ph})^{-1}$.

This means that, even if the two polaritons have mixed with each other during the short time stage of the evolution, the decay to the ground state occurs according to the dressed-state decay rate. In other words, the benefit of having an accelerated spontaneous emission persists even in the presence of strong dephasing. This result is the main outcome of our treatment.

6 Approximate analytical solution for the polariton decay under strong-coupling / moderate-dephasing conditions

In general, equations (13) (or (14)) lead to four eigenvalues, in addition to the trivial eigenvalue $\lambda = 0$ which contribute only to the ground state probability. Under the following conditions:

1) strong coupling $g \gg \kappa_{\rm ph}, \gamma_{\rm ex}$,

2) moderate dephasing $\gamma_\phi \stackrel{\sim}{<} g$,

it turns out that two of the four eigenvalues are real and two are complex. More importantly, we found that

a) when the initial condition correspond to a single initial lower or upper polariton, the two complex eigenvalues are irrelevant, in the sense that their contributions have negligible weight,

b) one can give an analytical approximation to the two real eigenvalues.

The two points a) and b), taken in combination, allow for giving an analytical approximation to the time evolution which works quite well for $\kappa_{\rm ph} > \gamma_{\rm ex}$ and $\delta > 0$ and remain qualitatively reasonable for $\delta < 0$. The analytical expressions for the two real eigenvalues are given by $\lambda_-^{\rm ap}$ of equation (24) and by

$$\overline{\lambda} = 2(\gamma_{\rm ex} + \gamma_\phi - \kappa_{\rm ph})\frac{g^2}{2\Delta^2} + 2\kappa_{\rm ph}\,; \qquad (25)$$

$\overline{\lambda}$ governs the short time evolution. Note that for $\delta \to \pm\infty$ and $\kappa_{\rm ph} > \gamma_{\rm ex}$ we have $\lambda_-^{\rm ap} \to 2\gamma_{\rm ex}$ and $\overline{\lambda} \to 2\kappa_{\rm ph}$. If, as usual, we call p_{10} and p_{01} the probabilities for the lower and the upper polariton, respectively, on the basis of a) and b) we can write

$$\begin{aligned} p_{10}(t) &= a e^{-\lambda_-^{\rm ap} t} + b e^{-\overline{\lambda} t}\,, \\ p_{01}(t) &= a' e^{-\lambda_-^{\rm ap} t} + b' e^{-\overline{\lambda} t}\,. \end{aligned} \qquad (26)$$

If initially there is a single lower polariton, we have $p_{10}(0) = 1$, $p_{01}(0) = 0$. In addition, from the second and the third of equations (14) we have that for $t = 0$

$$\begin{aligned} \frac{{\rm d}p_{10}}{{\rm d}t} &= -(2\gamma_1 + \gamma_\phi \frac{g^2}{2\Delta^2})\,, \\ \frac{{\rm d}p_{01}}{{\rm d}t} &= \gamma_\phi \frac{g^2}{2\Delta^2}\,, \end{aligned} \qquad (27)$$

so that, using equations (26) and (20), we obtain the result

$$a = \frac{\gamma_\phi g^2 + 2\delta(\Delta+\delta)(\kappa_{\rm ph}-\gamma_{\rm ex})}{2\delta^2(\kappa_{\rm ph}-\gamma_{\rm ex}) + 2\Delta^2\{(\gamma_{\rm ex}-\kappa_{\rm ph})^2 + R^2(\delta)\}^{1/2}}\,,$$
$$b = 1-a\,,$$
$$a' = \frac{\gamma_\phi g^2}{2\delta^2(\kappa_{\rm ph}-\gamma_{\rm ex}) + 2\Delta^2\{(\gamma_{\rm ex}-\kappa_{\rm ph})^2 + R^2(\delta)\}^{1/2}}\,,$$
$$b' = -a'\,, \qquad (28)$$

where $R^2(\delta)$ is given by the equation following (24).

It is interesting to see how this simple model fits the experimental data on the lower cavity-polariton decay time. Figure 8 presents a fit to the experimental data obtained in references [8,9]. In carrying out this calculation, the exciton decay rate $\gamma_{\rm ex}$ was assumed to be thermally activated and thus taken to depend on the exciton-cavity detuning in the form

$$\gamma_{\rm ex} = \gamma_{\rm ex}^{(0)} e^{-(\Delta-\delta)/kT}\,. \qquad (29)$$

Use of this form implies the assumption that $\gamma_{\rm ex}$ is dominated by the scattering of excitons to very large wave vectors, in regions of phase space where they cannot interact with light, as we discussed in Section 3. The energy of the lower cavity polariton before scattering is given by $-\Delta$ (with respect to $(\omega_{\rm ex}+\omega_{\rm ph})/2$), while the energy of the final state (which is unchanged by the presence of the cavity, since it does not interact with light) is given by $-\delta$. Thus, the energy $(\Delta-\delta)$ required in this scattering process is provided by thermal phonons. The parameters used in this fit are: $\tau_{\rm ex}^{(0)} \equiv (2\gamma_{\rm ex}^{(0)})^{-1} = 12$ ps, $\tau_{\rm ph} = 2.0$ ps, $2g = 4.4$ meV and $(\gamma_\phi)^{-1} = 5.5$ ps. The good quality of the fit seen in Figure 8, indicates that this model describes quite well the physics of the cavity polariton decay, in spite of its simplistic assumptions which consist essentially in lumping together the different wave vector states of the exciton and thus considering a "generic" Wannier exciton, as discussed in Section 2. It should be noticed that the dephasing time $T_2^* = \gamma_\phi^{-1}$ obtained in our fit is of the same order as that which can be deduced from measurements of the exciton decay time (T_1) and the total dephasing time (T_2) in coherent transient experiments in GaAs quantum wells [28].

7 Conclusions and comments

We have presented a simple model that describes the system of quantum well excitons in a planar microcavity. In treating the radiative interaction and the relaxation processes within this model, the different wave vector states of the exciton and of the cavity-confined photons are not distinguished separately, but are lumped together into a "generic" exciton and cavity-photon quasi-particles. This simplification, whose validity rests on the fact that in "leaky" semiconductor microcavities only small regions of the exciton and photon phase spaces interact strongly, permits us to use the traditional model of atomic physics to deal both with the strong radiative interaction that produces cavity polaritons and with the decay processes that the polaritons undergo because of the decay of their constituent excitons and cavity photons.

Within this model, we have been able to identify the main features which characterize the decay of a single polariton in the presence of scattering precesses leading to dephasing. In particular, we have found an analytical solution in a case which is interesting experimentally, namely under conditions of strong exciton-photon coupling such that the dephasing rate is smaller than the coupling. The results show that, in this case, the decay of the polariton occurs basically in two stages. During the first stage, the two kinds of polaritons get admixed, in the sense that if initially there is, *e.g.*, a pure lower polariton, in the course of time there is a finite probability of finding an upper polariton; this is a pure effect of dephasing since in the absence of dephasing a lower polariton remains a pure lower polariton all the time. In the second stage, the admixed polaritons decay together with a common rate. In the resonant case this decay rate is still quite close to the average of the decay rates of the two bare modes, which means that the spontaneous emission acceleration under strong-coupling conditions is robust with respect to dephasing.

We have used this model to fit experimental results on the decay time of the lower cavity polariton. The quality of the fit indicates that in spite of its severe simplifications, this model can provide a valid conceptual framework for treating quantum electrodynamic effects in semiconductor microcavities.

References

1. V. Savona, L.C. Andreani, P. Schwendimann, A. Quattropani, Solid State Commun. **93**, 733 (1994).
2. C. Weisbuch, M. Nishioka, A. Ishikawa, Y. Arakawa, Phys. Rev. Lett. **69**, 3314 (1992).
3. I. Abram, S. Iung, R. Kuszelewicz, G. LeRoux, C. Licoppe, J.L. Oudar, E.V.K. Rao, J.I. Bloch, R. Planel, V. Thierry-Mieg, Appl. Phys. Lett. **65**, 2516 (1994).
4. R. Houdré, C. Weisbuch, R.P. Stanley, U. Oesterle, P. Pellandini, M. Ilegems, Phys. Rev. Lett. **73**, 2043 (1994).
5. D.S. Citrin, IEEE J. Quantum Electron. **30**, 997 (1994).
6. S. Jorda, Phys. Rev. B **50**, 18690 (1994).
7. I. Abram, J.L. Oudar, Phys. Rev. A **51**, 4116 (1995).
8. I. Abram, B. Sermage, S. Long, J. Bloch, R. Planel, V. Thierry-Mieg, in *Microcavities and Photonic Bandgaps: Physics and Applications*, edited by J. Rarity and C. Weisbuch (Kluwer Academic Publ., 1996) p. 69.
9. B. Sermage, S. Long, I. Abram, J.Y. Marzin, J. Bloch, R. Planel, V. Thierry-Mieg, Phys. Rev. B **53**, 16516 (1996).
10. G. Björk, A. Karlsson, Y. Yamamoto, Phys. Rev. A **50**, 1675 (1994).
11. V. Savona, F. Tassone, C. Piermarocchi, A. Quattropani, P. Schwendimann, Phys. Rev. B **53**, 13051 (1996).
12. D. Oberhauser, K. -H. Pantke, J. M. Hvam, G. Weimann, C. Klingshirn, Phys. Rev. B **47**, 6827 (1993)
13. S. Pau, G. Björk, J. Jacobson, Y. Yamamoto, Nuovo Cimento D **17**, 1657 (1995)

14. V. Savona, F Tassone, C. Piermarocchi, A. Quattropani, P. Schwendimann, Phys. Rev. B **53**, R7642 (1996).
15. J. Bloch J.Y. Marzin, Phys. Rev. B **56**, 2103 (1997).
16. F. Tassone, C. Piermarocchi, V. Savona, A. Quattropani, P. Schwendimann, Phys. Rev. B **56**, 7554 (1997).
17. G. Björk, S. Pau, J.M. Jacobson, H. Cao, Y. Yamamoto, J. Opt. Soc. Am. B **13**, 1069 (1996).
18. V. Savona, C. Weisbuch, Phys. Rev. B **54**, 10835 (1996); D. Birkedal, V.G. Lyssenko, K.H. Pantke, J. Erland, J.M. Hvam, Phys. Rev. B **51**, 7977 (1995); R. Zimmermann, Nuovo Cimento D **17**, 1801 (1995)
19. F. Jahnke, M. Koch, T. Meier, J. Feldmann, W. Schäfer, P. Thomas, S.W. Koch, E.O Göbel, H. Nickel, Phys. Rev. B,**50**, 8144 (1994)
20. E. Hanamura, J. Inoue, F. Yura, J. Nonlinear Optics Phys. Mater. **4**, 13 (1995).
21. L.C. Andreani, in *Confined Electrons and Photons: New Physics and Devices*, edited by E. Burstein and C. Weisbuch (Plenum Press, 1995) p. 57.
22. D.S. Citrin, in *Confined Electrons and Photons: New Physics and Devices*, edited by E. Burstein and C. Weisbuch (Plenum Press, 1995) p. 205; D.S. Citrin, Comm. Cond. Mat. Phys., **16**, 263 (1993).
23. R. Bonifacio, F. Haake, Z. Phys. **200**, 527 (1967).
24. R.J. Glauber, Phys. Rev. **130**, 2529 (1963).
25. S. Pau, G. Bjork, J. Jacobson, H. Cao, Y. Yamamoto, Phys. Rev. A **51**, 14437 (1995).
26. T.B. Norris, J.K. Rhee, C.Y. Sung, Y. Arakawa, M. Nishioka, C. Weisbuch, Phys. Rev. B **50**, 14663 (1994).
27. P. Meystre, M. Sargent III, *Elements of Quantum Optics* (Springer-Verlag, Berlin 1991).
28. L. Schultheis, M.D. Sturge, J. Hegarty, Appl. Phys. Lett. **47**, 995 (1985).